TKYNT-07-04, UT-07-08

Stau-catalyzed ^{6}Li Production in Big-Bang Nucleosynthesis

K. Hamaguchi[1], T. Hatsuda[1], M. Kamimura[2], Y. Kino[3] and T. T. Yanagida[1]

[1] *Department of Physics, The University of Tokyo, Tokyo 113-0033, Japan*

[2] *Department of Physics, Kyushu University, Fukuoka 812-8581, Japan*

[3] *Department of Chemistry, Tohoku University, Sendai 980-8578, Japan*

Abstract

If the gravitino mass is in the region from a few GeV to a few 10's GeV, the scalar lepton X such as stau is most likely the next lightest supersymmetry particle. The negatively charged and long-lived X^- may form a Coulomb bound state (AX^-) with a nucleus A and may affect the big-bang nucleosynthesis through catalyzed fusion process. We calculate a production cross section of ^{6}Li from the catalyzed fusion $(^4\mathrm{He}X^-) + d \to {}^6\mathrm{Li} + X^-$ by solving the Schrödinger equation exactly for three-body system of ^{4}He, d and X. We utilize the state-of-the-art coupled-channel method, which is known to be very accurate to describe other three-body systems in nuclear and atomic reactions. The importance of the use of appropriate nuclear potential and the exact treatment of the quantum tunneling in the fusion process are emphasized. We find that the astrophysical S-factor at the Gamow peak corresponding to $T = 10$ keV is 0.038 MeV barn. This leads to the ^{6}Li abundance from the catalyzed process as $^6\mathrm{Li}|_{\mathrm{CBBN}} \simeq 4.3 \times 10^{-11} (\mathrm{D}/2.8 \times 10^{-5})([n_{X^-}/s]/10^{-16})$ in the limit of long lifetime of X. Particle physics implication of this result is also discussed.

I. INTRODUCTION

The gravitino is the most important prediction of supergravity (SUGRA) [1]. Its mass is expected to be in a wide range, 1 eV$-$100 TeV, depending on the mediation mechanism of supersymmetry (SUSY) breaking effects. In particular, the gravitino with a mass of $O(1)$ MeV$-O(10)$ GeV is very interesting in the sense that it is most likely the stable and lightest SUSY particle (LSP) and can be a candidate of cold dark matter in the universe. Moreover, if the gravitino mass lies between a few GeV and a few 10's GeV and the next LSP (NLSP) is a charged scalar lepton (X) such as stau ($\tilde{\tau}$), the SUGRA can be tested in high-energy collider experiments [2]. The key observation is that the gravitino mass $m_{3/2}$, the stau mass $m_{_X}$ and the stau lifetime $\tau_{_X}$ could be measured in high precision if $m_{3/2}$ is of $O(10)$ GeV (cf. [3]). Then the Planck scale $M_{\rm PL}$ is extracted through the relation, $\tau_{_X}^{(\rm exp.)} = \tau_{_X}(m_{_X}^{(\rm exp.)}, m_{3/2}^{(\rm exp.)}, M_{\rm PL})$. This independent determination of $M_{\rm PL}$ will provide us with a crucial test of the SUGRA.

For the gravitino mass in such an interesting region as discussed above, the stau has necessarily a long lifetime. For example, it is of order one month for $m_{3/2} \simeq 10$ GeV and $m_X \simeq 100$ GeV. However, such a long-lived particle is potentially dangerous in cosmology. If it decays after the big-bang nucleosynthesis (BBN), the decay products destroy the light elements and ruin the success of the SBBN (standard BBN) [4, 5]. More seriously, if the long-lived particle is negatively charged as X^-, it forms bound states together with positively charged nuclei, which leads to an enhancement of some nuclear reaction rates. That is, X^- plays as a catalyzer of nuclear fusion (catalyzed BBN or CBBN in short) and affects cosmological nuclear abundances.[1]

In a recent article [7], Pospelov has argued that too much ^{6}Li is produced through the CBBN if the lifetime of X^- is long enough, $\tau_{_X} > 10^3 - 10^4$ sec, and its abundance is large enough, $n_{_{X^-}}/s > 10^{-17}$, where $n_{_{X^-}}$ and s are the number density of X^- and the entropy density of the universe, respectively.[2] The production rate of ^{6}Li estimated in Ref. [7] is based on a naive comparison of the standard process $^4{\rm He}+d \to {}^6{\rm Li}+\gamma$ and the new catalyzed process $(^4{\rm He}X^-)+d \to {}^6{\rm Li}+X^-$ where $(^4{\rm He}X^-)$ is the 1s Coulomb bound state of ^{4}He and

[1] Massive and long-lived X^- produced in accelerators may be of practical use as a catalyzer for D-D and D-T fusions similar to the muon catalyzed fusion [6].

[2] Other effects of the X^- bound states have been considered in [8, 9].

X^-. It is assumed that the standard process is dominated by the E2 transition[3] induced by the interaction $Q_{ij}\nabla_i E_j$ with Q_{ij} being the quadrapole operator. Then, by applying the same interaction to the photonless process with E_j replaced by the Coulomb field associated with X^-, it was concluded that the astrophysical S-factor of the new process at zero incident energy is about 0.3 MeV barn. However, the assumptions adopted in the above estimate do not have firm ground: For example, the angular momentum of the initial ^{4}He-d system in the catalyzed process is dominated by zero, $L = 0$, while the angular momentum of the initial system in the standard process is dominated by $L = 2$ ($L = 1$) for the E2 (E1) transition. Such a kinematical difference invalidates the use of the SBBN process to estimate the CBBN process. Furthermore, the quantum interplay between the $^4\mathrm{He} - d$ nuclear fusion and the tunneling of d through the Coulomb barrier plays an important role in low-energy catalyzed fusion and cannot be treated in a perturbative manner.

The purpose of this paper is to solve the Shrödinger equation for the three-body system (^{4}He, d and X^-) exactly and derive a reliable S-factor for the X^- CBBN. The method we adopt is the state-of-the-art coupled-channel technique developed by two of the present authors (M.K. and Y.K.) together with E. Hiyama [11, 12, 13, 14]. Since we can treat the catalyzed process directly, we do not need to refer to any of the SBBN processes. Also, the method has been already proven to be highly accurate and useful in atomic and nuclear physics (reviewed in [14]). We find that the obtained astrophysical S-factor at $E = 36.4$ keV (the position of the Gamow peak for $T = 10$ keV which is relevant to the CBBN) is 0.038 MeV barn. This is about 10 times smaller than the estimate in Ref. [7] at the same energy. For long lived stau, our S-factor leads to the ^{6}Li abundance from CBBN as $^6\mathrm{Li}|_{\mathrm{CBBN}} \simeq 4.3 \times 10^{-11}(\mathrm{D}/2.8 \times 10^{-5})([n_{X^-}/s]/10^{-16})$. Therefore, an observational upper bound on the ^{6}Li abundance $^6\mathrm{Li} < 6.1\times10^{-11}$ (2σ) [5] leads to a bound on the X^- abundance, $n_{X^-}/s < 1.4 \times 10^{-16}$. This requires a dilution of the relic stau by some entropy production at late time by a factor of $\Delta \simeq (300 - 600) \times (m_{\tilde{\tau}}/100\ \mathrm{GeV})$. Such a dilution factor can easily be consistent with the thermal leptogenesis [15] for a reheating temperature $T_R \gtrsim 10^{12}$ GeV.

The organization of this paper is as follows. In Sec.II, we summarize the basic reaction of

[3] This particular assumption itself may not be justified since E1 transition could be comparable or even larger than E2 at low energies. See e.g. [10].

the X^- catalyzed fusion as well as its atomic analogue, the muon transfer reaction. In Sec.III, we present our method of solving the ^{4}He-d-X$^-$ three-body problem. In Sec.IV, we show our result of astrophysical S-factor as a function of the incident energy. Sec.V is devoted to conclusion and discussions in which the ^{6}Li abundance in CBBN and its implication to particle physics are also mentioned.

II. THE X^- CATALYZED PROCESS

As we have mentioned in the Introduction, we will treat the following process directly in a fully quantum mechanical manner:

$$(^4\mathrm{He}X^-) + d \rightarrow {}^6\mathrm{Li} + X^- + 1.1\,\mathrm{MeV}. \tag{2.1}$$

As shown later in Section V, the relevant temperature T for CBBN is about 10 keV. This corresponds to the Gamow peak of the incident channel located at the c.m. energy E_{G} =36.4 keV with the full $1/e$ width of 44 keV. Thus the c.m. energy of the incident channel will be typically up to 100 keV. We adopt the $^4\mathrm{He} - d$ cluster model in which the ^{6}Li nucleus is a bound state of a ^{4}He nucleus and a deuteron. This model has extensively been utilized in the studies of the structure and reactions of light nuclei and is very well established (see e.g. [16, 17]). Such a cluster-model treatment allows us to investigate the reaction (2.1) as a quantum three-body problem, $^4\mathrm{He} + d + X^-$. The rearrangement of the three ingredients takes place during the reaction process through the long range Coulomb interaction and the short range nuclear interaction.

Although solving the three-body problem accurately is quite an elaborate task, two of the authors (M.K. and Y.K.) have an experience [12, 13, 14] to have solved a similar subject, the muon transfer reaction,

$$(d\mu^-)_{1s} + t \rightarrow (t\mu^-)_{1s} + d + 48\ \mathrm{eV} \tag{2.2}$$

at incident energies of $0.001 - 100$ eV in the context of the muon catalyzed D-T fusion cycle [18]. Among the calculations of this reaction in the literatures, their three-body coupled-channel method was found to provide with the most accurate result (see §8 of [14]).

In the present paper, the same coupled-channel method is applied to the reaction, Eq. (2.1). We note here that it is very important to employ an appropriate nuclear interaction

between ^{4}He and deuteron in treating the reaction; we choose the interaction which can reproduce the binding energy and the charge form-factor of ^{6}Li as well as the low-energy $^4\mathrm{He}-d$ scattering phase shift.

III. COUPLED CHANNEL METHOD

Following Ref.[14], we briefly explain the three-body coupled-channel method to investigate the reaction (2.1). As shown in Fig.1, we consider all the Jacobi coordinates $(\mathbf{r}_c, \mathbf{R}_c)$ of the three possible sets, $c = 1, 2$ and 3. The entrance channel $(^4\mathrm{He}X^-) + d$ and the exit channel $^6\mathrm{Li} + X^-$ in our reaction are best described by the coordinates for $c = 1$ and those for $c = 2$, respectively. Since we are interested in the incident energy of the entrance channel below 100 keV, there is no other open channel than the above two. All the excited states of $(^4\mathrm{He}X^-)$ and ^{6}Li as well as all the states of (dX^-) can be excited only virtually in the intermediate stage of the reaction. To describe such an intermediate state where particle-rearrangement takes place, it is convenient to utilize the coordinates for $c = 3$ together with those for $c = 1, 2$.

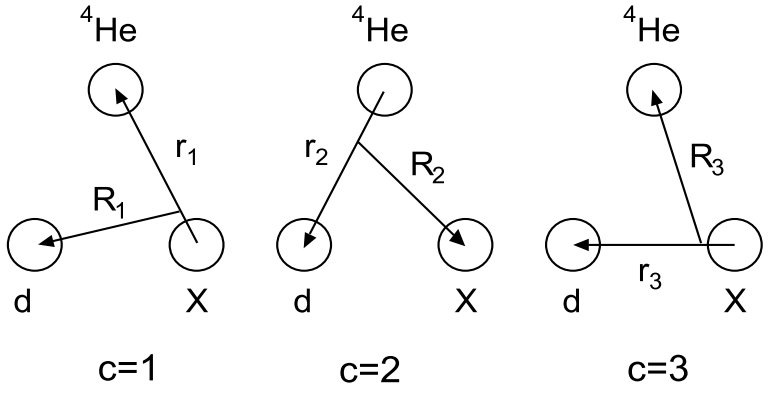

FIG. 1: Three sets of Jacobi coordinates of the $^4\mathrm{He} + d + X^-$ system. The entrance (exit) channel is described by the coordinate system of $c = 1$ ($c = 2$).

A. Three-body Schrödinger equation

The Schrödinger equation for the total wave function Ψ_{JM} of the ${}^4\mathrm{He} + d + X^-$ system having an angular momentum J and its z-component M is given by

$$(H - E_{\rm tot})\Psi_{JM} = 0, \tag{3.1}$$

with the Hamiltonian,

$$H = -\frac{\hbar^2}{2m_c}\nabla^2_{\mathbf{r}_c} - \frac{\hbar^2}{2M_c}\nabla^2_{\mathbf{R}_c} + V_{^4\mathrm{He}\text{-}X}(r_1) + V_{^4\mathrm{He}\text{-}d}(r_2) + V_{d\text{-}X}(r_3). \tag{3.2}$$

As far as we use the reduced masses (m_c and M_c) associated with the coordinates ($\mathbf{r}_c$ and $\mathbf{R}_c$), every choice of c in the kinetic term is equivalent. $V_{A_c\text{-}B_c}(r_c)$ denotes the potential between the particles A_c and B_c (A_1-$B_1 = {}^4\mathrm{He}$-X, A_2-$B_2 = {}^4\mathrm{He}$-d, A_3-$B_3 = d$-X) and will explicitly be given below.

Spin of the deuteron is neglected, and therefore the angular momentum of the ground states of ${}^6\mathrm{Li}$ is zero as well as that of $({}^4\mathrm{He}X^-)$. We denote the ground-state wave function of $({}^4\mathrm{He}X^-)$ in $c = 1$ by $\phi^{(1)}_{\rm g.s.}(\mathbf{r}_1)$ and its eigenenergy by $\varepsilon^{(1)}_{\rm g.s.}$, and similarly, that of ${}^6\mathrm{Li}$ in $c = 2$ by $\phi^{(2)}_{\rm g.s.}(\mathbf{r}_2)$ and its eigenenergy by $\varepsilon^{(2)}_{\rm g.s.}$. They are obtained by solving

$$[\,-\frac{\hbar^2}{2m_c}\nabla^2_{\mathbf{r}_c} + V_{A_c\text{-}B_c}(r_c) - \varepsilon^{(c)}_{\rm g.s.}\,]\,\phi^{(c)}_{\rm g.s.}(\mathbf{r}_c) = 0. \qquad (c = 1, 2) \tag{3.3}$$

Center-of-mass scattering energy of the channel c associated with the coordinate $\mathbf{R}_c$, say E_c, is introduced by $E_c = E_{\rm tot} - \varepsilon^{(c)}_{\rm g.s.}$ together with the corresponding wave number k_c by $\hbar^2 k_c^2/2M_c = E_c\,(c = 1, 2)$. For a given total energy $E_{\rm tot}$, the Schrödinger equation (3.1) should be solved under the scattering boundary condition:

$$\lim_{R_c\to\infty}\Psi_{JM} = \phi^{(c)}_{\rm g.s.}(\mathbf{r}_c)\Big[u^{(-)}_J(k_cR_c)\delta_{c\,1} - \sqrt{\frac{v_1}{v_c}}S^J_{1\to c}u^{(+)}_J(k_cR_c)\Big]Y_{JM}(\widehat{\mathbf{R}}_c), \qquad (c = 1, 2) \tag{3.4}$$

where $u^{(\pm)}_J(kR)(= (G_J(kR) \pm iF_J(kR))/kR)$ are the asymptotic outgoing and incident Coulomb wave functions. $S^J_{1\to c}$ is the S-matrix for the transition from the channel 1 to c and v_c is the velocity of the channel c. By introducing a simplified notation, $E \equiv E_1$ and $k \equiv k_1$, the cross section of the rearrangement process (2.1) is given by

$$\sigma_{1\to 2}(E) = \frac{\pi}{k^2}\sum_{J=0}^{\infty}(2J+1)|S^J_{1\to 2}|^2, \tag{3.5}$$

and the astrophysical S-factor is derived from

$$S(E) = \sigma_{1\to 2}(E)\, E \exp(2\pi\eta(E)), \tag{3.6}$$

where $\eta(E)$ is the Sommerfeld parameter of the entrance channel.

The three-body wave function which describes the transfer reaction (2.1) and the elastic $(^4\mathrm{He}X^-) + d$ scattering simultaneously is written as

$$\Psi_{JM} = \phi^{(1)}_{\mathrm{g.s.}}(\mathbf{r}_1)\, \chi^{(1)}_{JM}(\mathbf{R}_1) + \phi^{(2)}_{\mathrm{g.s.}}(\mathbf{r}_2)\, \chi^{(2)}_{JM}(\mathbf{R}_2) + \Psi^{(\mathrm{closed})}_{JM} \ . \tag{3.7}$$

The first and the second terms represent the open channels, $c = 1$ for $(^4\mathrm{He}X^-) + d$ and $c = 2$ for $^6\mathrm{Li} + X^-$. The factors $\chi^{(c)}_{JM}(\mathbf{R}_c)(= \chi^{(c)}_J(R_c)\, Y_{JM}(\widehat{\mathbf{R}}_c)\,)$ describe the scattering waves along the coordinates $\mathbf{R}_c$ and are to be solved under the boundary condition (3.4). The third term, $\Psi^{(\mathrm{closed})}_{JM}$, stands for all the closed (virtually-excited) channels in the energy range of this work; in other words, this term is introduced to represent all the asymptotically-vanishing three-body amplitudes that are not included in the first two scattering terms. For example, the third term describes such an effect that the incoming deuteron attracts the ^{4}He in the 1s-orbit around X^- and distorts the orbit before picking up the ^{4}He.

Since $\Psi^{(\mathrm{closed})}_{JM}$ vanishes asymptotically, it is reasonable and useful [12, 13, 14] to expand it in terms of a complete set of L^2-integrable three-body basis functions, $\{\Phi_{JM,\nu}; \nu = 1-\nu_{\max}\}$, spanned in a finite spatial region (see Sec.3.C):

$$\Psi^{(\mathrm{closed})}_{JM} = \sum_{\nu=1}^{\nu_{\max}} b_{J\,\nu}\ \Phi_{JM,\,\nu}. \tag{3.8}$$

Equations for $\chi^{(1)}_J(R_1)$, $\chi^{(2)}_J(R_2)$ and the coefficient $b_{J\nu}$ are given by the $\nu_{\max}+2$ simultaneous equations

$$\langle\, \phi^{(c)}_{\mathrm{g.s.}}(\mathbf{r}_c) Y_{JM}(\widehat{\mathbf{R}}_c)\ \,|\, H - E_{\mathrm{tot}} \,|\, \Psi_{JM}\,\rangle_{\mathbf{r}_c,\,\widehat{\mathbf{R}}_c} = 0, \qquad (c = 1, 2) \tag{3.9}$$

and

$$\langle\, \Phi_{JM,\,\nu} \,|\, H - E_{\mathrm{tot}} \,|\, \Psi_{JM}\,\rangle = 0. \qquad (\nu = 1 - \nu_{\max}) \tag{3.10}$$

Here, $\langle\quad\rangle_{\mathbf{r}_c,\,\widehat{\mathbf{R}}_c}$ denotes the integration over $\mathbf{r}_c$ and $\widehat{\mathbf{R}}_c$.

Since $\Phi_{JM,\,\nu}$ are constructed so as to diagonalize the three-body Hamiltonian as

$$\langle \Phi_{JM,\nu}|\, H\, |\Phi_{JM,\nu'}\rangle = E_{J\,\nu}\delta_{\nu\nu'}, \qquad (\nu, \nu' = 1 - \nu_{\max}) \tag{3.11}$$

the coefficients $b_{J\nu}$ can be written, from Eqs.(3.10), as

$$b_{J\nu} = \frac{-1}{E_{J\nu} - E_{\mathrm{tot}}} \langle \Phi_{JM,\,\nu} \,|\, H - E_{\mathrm{tot}} \,|\, \phi^{(1)}_{\mathrm{g.s.}}\chi^{(1)}_{JM} + \phi^{(2)}_{\mathrm{g.s.}}\chi^{(2)}_{JM}\rangle. \qquad (\nu = 1 - \nu_{\max}) \tag{3.12}$$

Inserting Eqs.(3.12) into $b_{J\nu}$ in Ψ_{JM} in Eqs.(3.9), we reach two coupled integro-differential equations for $\chi_J^{(1)}(R_1)$ and $\chi_J^{(2)}(R_2)$.

The integro-differential equations, though not recapitulated here (c.f. §8 of [14] for them), are solved by using both the direct numerical method (finite-difference method) and the Kohn-type variational method [14, 19], and we have obtained the same result for the incident energies relevant to CBBN, $E > 10$ keV. The coupling between the entrance and exit channels as well as the contribution from the closed channels $\Psi_{JM}^{(\mathrm{closed})}$ were found to be significantly large as will be discussed later.

B. Nuclear potentials

It is essential for the three-body calculation to employ appropriate nuclear interaction between ^{4}He and deuteron which governs the ^{4}He-transfer process. In this subsection, we define the potentials $V_{^4\mathrm{He}\text{-}X}(r_1), V_{^4\mathrm{He}\text{-}d}(r_2)$ and $V_{d\text{-}X}(r_3)$ in our Hamiltonian (3.2). First, we assume Gaussian-shape charge distributions of ^{4}He and deuteron as $2e(\pi b_1^2)^{-3/2}\mathrm{e}^{-(r/b_1)^2}$ and $e(\pi b_3^2)^{-3/2}\mathrm{e}^{-(r/b_3)^2}$, respectively. We take $b_1 = 1.37$ fm and $b_3 = 1.75$ fm, which reproduce observed r.m.s. charge radii, 1.68 fm of ^{4}He and 2.14 fm of deuteron. The potential between ^{4}He and X^- is then given by

$$V_{^4\mathrm{He}\text{-}X}(r_1) = -\,2\,e^2\,\frac{\mathrm{erf}(r_1/b_1)}{r_1}, \tag{3.13}$$

and that between deuteron and X^- is written as

$$V_{d\text{-}X}(r_3) = -\,e^2\,\frac{\mathrm{erf}(r_3/b_3)}{r_3}, \tag{3.14}$$

where $\mathrm{erf}(x) = \frac{2}{\sqrt{\pi}}\int_0^x e^{-t^2}\mathrm{d}t$ is the error function. Energy of the $(^4\mathrm{He}X^-)_{1s}$ state is $\varepsilon_{\mathrm{g.s.}}^{(1)} = -337.33$ keV and the r.m.s. radius is $\langle\, r_1^2\,\rangle^{1/2} = 6.84$ fm.

The potential $V_{^4\mathrm{He}\text{-}d}(r_2)$ is a sum of the nuclear potential, $V_{^4\mathrm{He}\text{-}d}^{\mathrm{N}}(r_2)$, and the Coulomb potential, $V_{^4\mathrm{He}\text{-}d}^{\mathrm{C}}(r_2)$. The latter is given by

$$V_{^4\mathrm{He}\text{-}d}^{\mathrm{C}}(r_2) = 2\,e^2\,\frac{\mathrm{erf}(r_2/\sqrt{b_1^2+b_3^2})}{r_2}. \tag{3.15}$$

The nuclear potential is assumed to have a two-range Gaussian shape as

$$V_{^4\mathrm{He}\text{-}d}^{\mathrm{N}}(r_2) = v_0\,e^{-(r_2/a)^2} + v_0'\,e^{-(r_2/a')^2} \tag{3.16}$$

with $a = 0.9$ fm, $v_0 = 500.0$ MeV, $a' = 2.0$ fm and $v'_0 = -64.06$ MeV. The first term, a repulsive core, is introduced to simulate the Pauli exclusion principle that nucleons in the incoming deuteron should not occupy the nucleon s-orbit in the ^{4}He nucleus during the reaction process (see e.g. [16] for this role of Pauli principle).

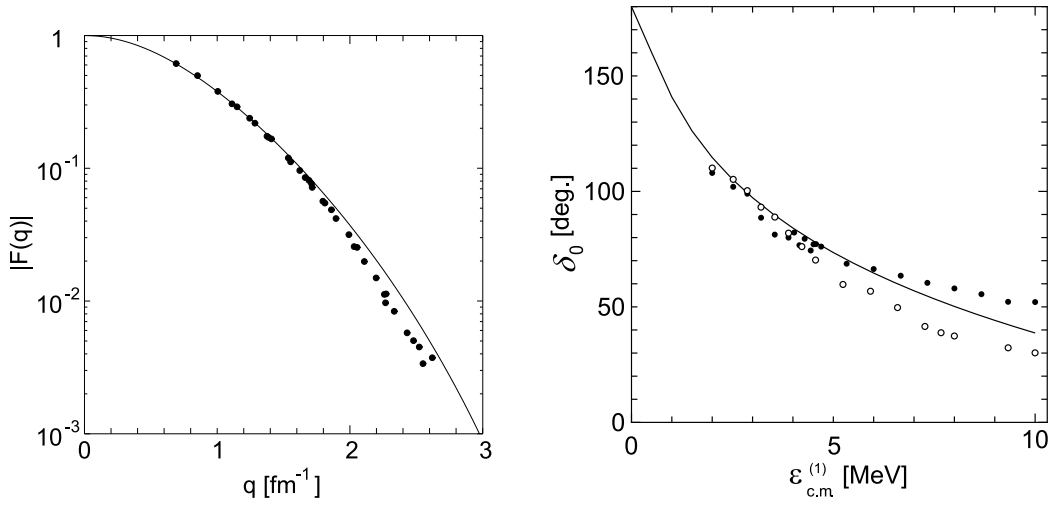

FIG. 2: Left panel: Charge form factor of the electron scattering from ^{6}Li. The calculated values (experimental data [20]) are shown by the solid line (filled circles). Right panel: The s-wave phase shift δ_0 of the $^4\mathrm{He} + d$ scattering at c.m. energy $\varepsilon^{(1)}_{\rm c.m.} < 10$ MeV. The calculated values are shown by the solid line, while the data from the phase-shift analysis are shown by filled circles [21] and by open circles [22].

The above parameters of $V^{\rm N}_{^4\mathrm{He}\text{-}d}(r_2)$ were so determined that the solution to the Schrödinger equation (3.3) could reproduce observed values of the energy $\varepsilon^{(2)}_{\rm g.s.} = -1.474$ MeV and the r.m.s. charge radius 2.54 fm of the ground state of ^{6}Li. Furthermore, the charge density of ^{6}Li reproduces observed charge form factor of the electron scattering from ^{6}Li as shown in the left panel of Fig.2. Simultaneously, use of the potential $V_{^4\mathrm{He}\text{-}d}(r_2)$ explains the low-energy s-wave phase shifts of the $^4\mathrm{He}+d$ scattering as shown in the right panel of Fig.2. Here, it should be noted that simple attractive potential without a repulsive core leads to the phase shift which increases with increasing E and cannot explain the observed data. We thus have a good $^4\mathrm{He} - d$ potential $V_{^4\mathrm{He}\text{-}d}(r_2)$ in order to perform a precise study of the three-body reaction (2.1). The potential $V_{^4\mathrm{He}\text{-}d}(r_2)$ and the wave function $\phi^{(2)}_{\rm g.s.}(r_2)$ are illustrated in Fig.3 in which r_2 is denoted by r for simplicity.

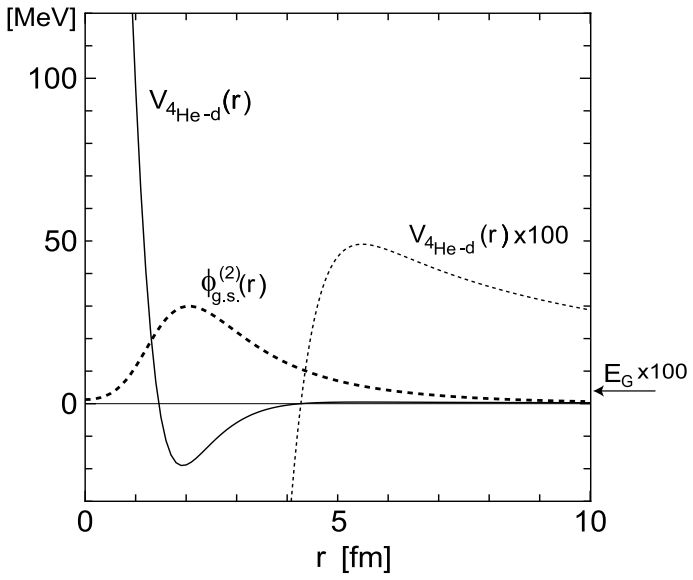

FIG. 3: The potential $V_{^4\mathrm{He}\text{-}d}(r)$ between ^{4}He and deuteron (the solid line). To show its Coulomb barrier tail, the same potential scaled by 100 is shown by the dotted line together with the typical incident kinetic energy $E_{\mathrm{G}} \times 100$ denoted by the arrow. The dashed line shows the $^4\mathrm{He} - d$ relative wave function in the ^{6}Li ground state in an arbitrary unit, $\phi^{(2)}_{\mathrm{g.s.}}(r)$.

C. Three-body basis functions

The L^2-integrable three-body basis functions $\{\Phi_{JM,\nu}; \nu = 1 - \nu_{\max}\}$ used in (3.8) to expand $\Psi^{(\mathrm{closed})}_{JM}$ are introduced as follows [14]: $\Phi_{JM,\nu}$ are written as a sum of the component functions in the Jacobi-coordinate sets $c = 1 - 3$ (Fig.1),

$$\Phi_{JM,\nu} = \Phi^{(1)}_{JM,\nu}(\mathbf{r}_1, \mathbf{R}_1) + \Phi^{(2)}_{JM,\nu}(\mathbf{r}_2, \mathbf{R}_2) + \Phi^{(3)}_{JM,\nu}(\mathbf{r}_3, \mathbf{R}_3) \ . \tag{3.17}$$

Each component is expanded in terms of the Gaussian basis functions of the coordinates $\mathbf{r}_c$ and $\mathbf{R}_c$:

$$\Phi^{(c)}_{JM,\nu}(\mathbf{r}_c, \mathbf{R}_c) = \sum_{n_c l_c, N_c L_c} A^{(c)}_{J\nu, n_c l_c, N_c L_c} \left[\phi^{\mathrm{G}}_{n_c l_c}(\mathbf{r}_c)\, \psi^{\mathrm{G}}_{N_c L_c}(\mathbf{R}_c)\right]_{JM} \qquad (c = 1 - 3) \ , \tag{3.18}$$

where

$$\phi^{\mathrm{G}}_{nlm}(\mathbf{r}) = r^l\, e^{-(r/r_n)^2}\, Y_{lm}(\widehat{\mathbf{r}}), \qquad r_n = r_1\, a^{n-1}, \qquad (n = 1 - n_{\max}) \tag{3.19}$$

$$\psi^{\mathrm{G}}_{NLM}(\mathbf{R}) = R^L\, e^{-(R/R_N)^2}\, Y_{LM}(\widehat{\mathbf{R}}), \quad R_N = R_1\, A^{N-1}, \quad (N = 1 - N_{\max}) \tag{3.20}$$

The Gaussian ranges are postulated to lie in geometric progression. Basis functions so chosen are suited for describing both short range correlations (mainly due to the $^4\mathrm{He} - d$

nuclear interaction) and long range asymptotic behavior simultaneously [14], and therefore they are efficient to describe the three-body configurations (closed-channel contribution) in the interaction region in the intermediate stage of reactions [12, 13, 14]. The coefficients $A^{(c)}_{J\nu,\,n_c l_c,\,N_c L_c}$ in (3.18) are determined by diagonalizing the three-body Hamiltonian H as Eqs.(3.11).

In the calculation for $J = 0$, we took $l_c = L_c = 0, 1, 2$ and $n_{\max} = N_{\max} = 15$ for $c = 1-3$. Therefore, total number of the three-body Gaussian basis functions $\left[\phi^{\rm G}_{n_c l_c}(\mathbf{r}_c)\,\psi^{\rm G}_{N_c L_c}(\mathbf{R}_c)\right]_{JM}$ to construct $\{\Phi_{JM,\nu}\}$ amounts to $\nu_{\max} = 2025$, which was found to be large enough for the present calculation. As for the Gaussian ranges, we took $r_1, r_{n_{\max}}, R_1$ and $R_{N_{\max}}$ to be 0.5, 15.0, 1.0, 40.0 fm, which are sufficiently precise for the present purpose. The expansion (3.8) was found to converge quickly with increasing ν, and $\nu \lesssim 100$ ($E_{J\nu} \lesssim 1$ MeV above the $(^4{\rm He}X^-) - d$ threshold) is very sufficient.

IV. RESULT OF THE REACTION RATE

Table I lists the cross section $\sigma_{1\to 2}(E)$ and the astrophysical S-factor $S(E)$ of the reaction (2.1) obtained by the full coupled-channel calculation at several energies around $E_{\rm G} = 36.4$ keV. In Fig.4, $S(E)$ is shown together with the Gamow peak. The S-factor increases with decreasing energy E since there are three-body bound states below the ^{6}Li-X^- threshold. Note that $S(E_{\rm G})$ estimated in [7] is an order of magnitude larger than the value given by the present exact calculation.

Since the S-factor can be approximated around $E_{\rm G}$ as

$$S(E) \simeq S(E_{\rm G}) + a\,(E - E_{\rm G}), \tag{4.1}$$

with $a = (\partial S/\partial E)_{E_{\rm G}}$, the reaction rate, using Eqs.(4.56) and (4.74) of [23], is expressed as

$$N_A\,\langle\,\sigma v\,\rangle = 6.24\times 10^9\,S(E_{\rm G})\,(1-0.0718\,a\,T_9/S(E_{\rm G}))\,T_9^{-2/3}\exp\left(-5.33\,T_9^{-1/3}\right)\ \ {\rm cm^3\,s^{-1}\,mol^{-1}}, \tag{4.2}$$

where N_A is the Avogadro constant and $S(E_{\rm G})$, a and T_9 are to be given in units of MeV barn, barn and 10^9 K, respectively. Taking $S(E_{\rm G}) = 0.0380$ MeV barn and $a = -0.18$ barn, we obtain

$$N_A\,\langle\,\sigma v\,\rangle = 2.37\times 10^8\,(1 - 0.34\,T_9)\,T_9^{-2/3}\exp\left(-5.33\,T_9^{-1/3}\right)\quad {\rm cm^3\,s^{-1}\,mol^{-1}}. \tag{4.3}$$

TABLE I: The cross section $\sigma_{1\to 2}(E)$ and the astrophysical S-factor $S(E)$ of the reaction $(^4\mathrm{He}X^-)+d\to {}^6\mathrm{Li}+X^-$ obtained by the full coupled-channel calculation. The most effective energy E_G for T =10 keV is 36.4 keV.

E [keV]	$\sigma_{1\to 2}$ [barn]	S [MeV barn]
10	3.85×10^{-6}	0.0426
20	1.09×10^{-4}	0.0410
36.4	6.88×10^{-4}	0.0380
50	1.41×10^{-3}	0.0357
100	3.50×10^{-3}	0.0286

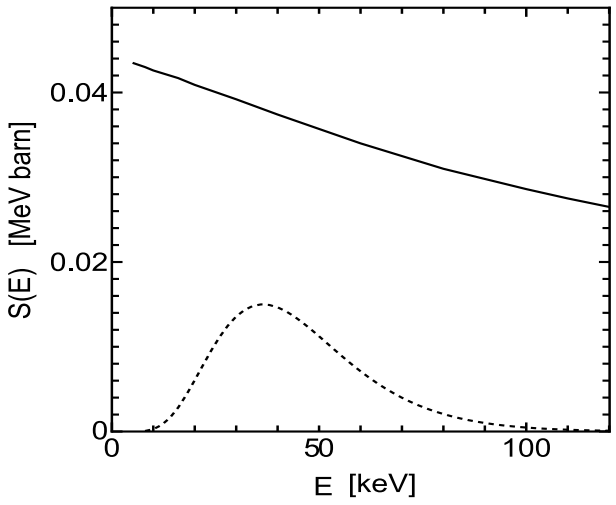

FIG. 4: The astrophysical S-factor (the solid line) obtained by the full coupled-channel calculation. The dashed line illustrates the Gamow peak (in arbitrary units) for T = 10 keV with the peak maximum at E_G = 36.4 keV.

To check the necessity of the exact coupled-channel treatment (3.7)−(3.12), we have calculated the cross sections in the following approximations: (i) A coupled-channel treatment with only the entrance and exit channels where the closed channel $\Psi_{JM}^{(\mathrm{closed})}$ in Eq.(3.7) is neglected, and (ii) an one-step approximation where the transition from the entrance channel

to the exit channel in the case (i) is treated in the leading order perturbation. For the case (i), the cross section $\sigma_{1\to 2}$ become approximately 3 times smaller than those in Table I. For the case (ii), the cross section becomes an order of magnitude larger than that in the case (i). Therefore, these approximations are not justified.

We have also checked that the cross section $\sigma_{1\to 2}$ is dominated by the total orbital angular momentum $J = 0$, and contribution from the higher angular momenta $J \geq 1$ is three orders of magnitude smaller. Furthermore, any pair among ^{4}He, d and X^- has dominantly zero orbital angular momentum, i.e. s-wave. This is in sharp contrast to the SBBN reaction $^4\mathrm{He} + d \to {}^6\mathrm{Li} + \gamma$ where the entrance channel is dominated either by d-wave (the E2 transition) or by p-wave (the E1 transition) from the selection rule.

V. CONCLUSIONS AND DISCUSSION

Since we consider the gravitino masses of order 10 GeV, the scalar lepton X (such as stau) is most likely the next lightest supersymmetry particle and could have a long lifetime more than 10^3 sec. Thus, the negatively charged X^- forms a bound states (AX^-) with positively charged nuclei A during the big-bang nucleosynthesis (BBN). Then, some nuclear abundances are enhanced through the catalyzed process.

In this Letter, we have calculated a production cross section of ^{6}Li from the catalyzed process $(^4\mathrm{He}X^-) + d \to {}^6\mathrm{Li} + X^-$ by exactly solving the Schrödinger equation for three-body system of ^{4}He, d and X. We utilize the state-of-the-art coupled-channel method, which is known to be very accurate to describe other three-body systems in nuclear and atomic reactions. The use of appropriate nuclear potential and the exact treatment of the quantum tunneling in the fusion process turned out to be important. We have found that the astrophysical S-factor at the Gamow peak corresponding to $T = 10$ keV is 0.038 MeV barn as shown in Table I, Fig. 4 and Eq. (4.3). They are the main results of this Letter.

Before closing, let us briefly discuss the particle physics implication of our result. With the cross section $\langle\, \sigma v \,\rangle$ in Eq. (4.3), the ^{6}Li production via CBBN is described by

$$\left.\frac{d}{dt}\,{}^6\mathrm{Li}\right|_{\mathrm{CBBN}} \;=\; n_{\mathrm{BS}} \langle\, \sigma v \,\rangle \mathrm{D}, \tag{5.1}$$

where $\mathrm{D} \equiv n_d/n_B$ and ${}^6\mathrm{Li} \equiv n_{^6\mathrm{Li}}/n_B$ are the abundances of these elements normalized by the baryon number density. The ratio of the number density of the bound states n_{BS} to the

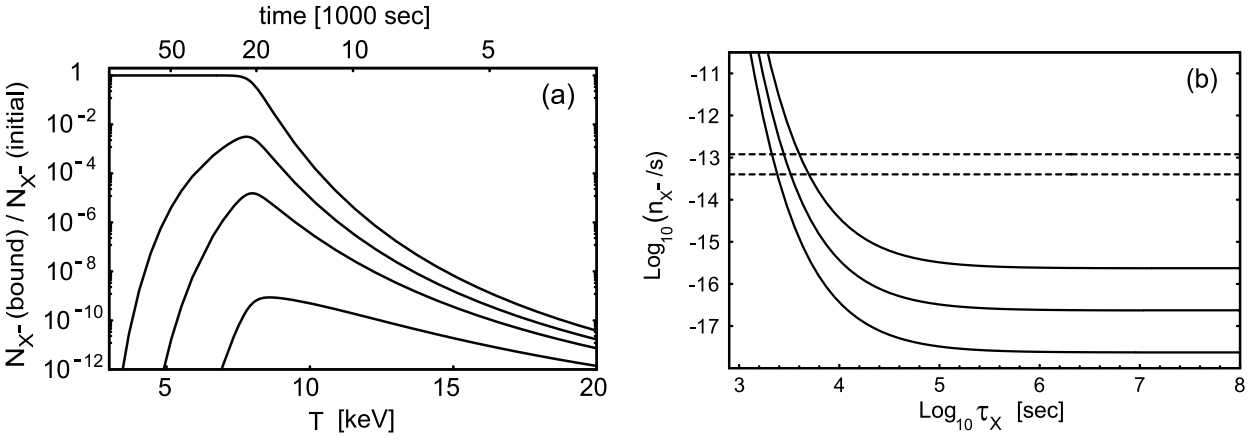

FIG. 5: (a) The number fraction of X^- particles which form bound states with ^{4}He as a function of temperature T. $\tau_X = (1, 2, 4, \infty) \times 10^3$ sec from bottom to top. (b) The contour plot of ^{6}Li abundance produced by the CBBN process in (τ_X, n_{X^-}/s) plane. The solid lines represent $^6\mathrm{Li} = 10^{-12}$, 10^{-11}, and 10^{-10} from the bottom to the top. The dashed lines represent the thermal relic abundance of stau for $m_{\tilde{\tau}} = 100$ GeV (below) and 300 GeV (above).

entropy density is given by [4]

$$\frac{n_{\rm BS}}{s} = \left.\frac{n_{X^-}}{s}\right|_{\rm initial} \cdot \frac{\exp(-t/\tau_X)}{1 + n_\alpha^{-1}(m_\alpha T/2\pi)^{3/2}\exp(-E_b/T)}, \tag{5.2}$$

where n_α and m_α are the number density and the mass of the ^{4}He, and E_b GeV is the binding energy of ($^4\mathrm{He}X^-$). The fraction of X^- which form bound states with ^{4}He is shown in Fig. 5(a), as a function of temperature T for various lifetimes of X.[5] The bound state abundance is peaked at around $T = 10$ keV for $\tau_X > 1000$ sec,[6] which justifies the expansion in Eq.(4.1). Thus, the CBBN occurs at $t \gg 1000$ sec, when the SBBN processes ($t < 1000$ sec) are already frozen. At such late time, the effect of the dissociation $^6\mathrm{Li} + p \rightarrow ^3\mathrm{He} + ^6\mathrm{He}$ is also negligible [5], and hence we have neglected it in Eq. (5.1).

Fig. 5(b) shows the contour plot of ^{6}Li abundance produced by the CBBN process, as a function of initial X^- abundance n_{X^-}/s and the lifetime τ_X. In the limit of long lifetime,

[4] We have assumed that the reaction $^4\mathrm{He} + X^- \leftrightarrow (^4\mathrm{He}X^-)$ is in chemical equilibrium. For more detailed analysis of the evolution of the bound state abundance, see Ref. [8].

[5] For our numerical calculation, we use $Y = 4n_\alpha/n_B = 0.25$, $\mathrm{D} = 2.78 \times 10^{-5}$, $n_B/s = 0.87 \times 10^{-10}$, $s = 1.715T^3$, $m_\alpha = 3.73$ GeV [24] and $E_b = 337.33$ GeV (see the previous section).

[6] For $\tau_X < 1000$ sec the CBBN effect is negligible. See Fig. 5(b).

one obtains

$$^6\mathrm{Li}\Big|_{\mathrm{CBBN}} \simeq 4.3 \times 10^{-11} \left(\frac{n_{X^-}/s}{10^{-16}}\right) \left(\frac{\mathrm{D}}{2.78 \times 10^{-5}}\right) . \tag{5.3}$$

Therefore, the observational upper bound on the ^{6}Li abundance $^6\mathrm{Li} < 6.1 \times 10^{-11}$ (2σ) [5] leads to a bound on the X^- abundance, $n_{X^-}/s < 1.4 \times 10^{-16}$. On the other hand, the thermal relic abundance of stau is given by $n_{\tilde{\tau}^-}/s \simeq (4-8) \times 10^{-14} (m_{\tilde{\tau}}/100\ \mathrm{GeV})$ [25]. (Conservative cases are shown in Fig. 5(b) as the dashed lines for $m_{\tilde{\tau}} = 100$ GeV and 300 GeV). Therefore, in the limit of long life time, an entropy production with a dilution factor $\Delta \simeq (300-600) \times (m_{\tilde{\tau}}/100\ \mathrm{GeV})$ for the primordial stau abundance is necessary to avoid the overproduction of ^{6}Li.[7]

On the other hand, this means that the primordial baryon asymmetry is also diluted by Δ. Standard thermal leptogenesis [15], an attractive mechanism for baryogenesis, can normally explain the observed baryon asymmetry if the reheating temperature satisfies $T_R \gtrsim 2 \times 10^9$ GeV [27]. Since the maximal baryon asymmetry is proportional to T_R in thermal leptogenesis, this means that, for a late time dilution $\Delta \simeq (300-600) \times (m_{\tilde{\tau}}/100\ \mathrm{GeV})$, the reheating temperature of $T_R \gtrsim (0.6-1.2) \times 10^{12}\ \mathrm{GeV} \times (m_{\tilde{\tau}}/100\ \mathrm{GeV})$ is necessary. Such a reheating temperature can be obtained in inflationary models.

Acknowledgments

T.H., M.K. and Y.K. were partly supported by the Grant-in-Aid of MEXT No. 18540253. Useful discussions with Emiko Hiyama are gratefully acknowledged.

---

[1] D. Z. Freedman, P. van Nieuwenhuizen and S. Ferrara, Phys. Rev. D **13** (1976) 3214; S. Deser and B. Zumino, Phys. Lett. B **62** (1976) 335.

[2] W. Buchmuller, K. Hamaguchi, M. Ratz and T. Yanagida, Phys. Lett. B **588**, 90 (2004) [arXiv:hep-ph/0402179].

[3] H. U. Martyn, Eur. Phys. J. C **48** (2006) 15 [arXiv:hep-ph/0605257]; K. Hamaguchi, M. M. Nojiri and A. de Roeck, arXiv:hep-ph/0612060.

[7] With this dilution factor, the masses of stau and gravitino considered here become also consistent with other BBN constraints [26].

[4] S. Weinberg, Phys. Rev. Lett. **48** (1982) 1303.

[5] M. Kawasaki, K. Kohri and T. Moroi, Phys. Rev. D **71** (2005) 083502 [arXiv:astro-ph/0408426].

[6] K. Hamaguchi, T. Hatsuda and T. T. Yanagida, arXiv:hep-ph/0607256.

[7] M. Pospelov, arXiv:hep-ph/0605215.

[8] K. Kohri and F. Takayama, arXiv:hep-ph/0605243;

[9] M. Kaplinghat and A. Rajaraman, Phys. Rev. D **74** (2006) 103004 [arXiv:astro-ph/0606209].

[10] K. M. Nollett, R. B. Wiringa and R. Schiavilla, Phys. Rev. C **63** (2001) 024003 [arXiv:nucl-th/0006064].

[11] M. Kamimura, Phys. Rev. **A38**, 621 (1988).

[12] M. Kamimura, Muon Catalyzed Fusion **3**, 335 (1988).

[13] Y. Kino and M. Kamimura, Hyperfine Interactions, **82**, 45 (1993).

[14] E. Hiyama, Y. Kino and M. Kamimura, Prog. Part. Nucl. Phys. **51** (2003) 223.

[15] M. Fukugita and T. Yanagida, Phys. Lett. B **174** (1986) 45.

[16] K. Ikeda *et al.*, Prog. Theor. Phys. Suppl. **68**, 1 (1980).

[17] M. Kamimura *et al.*, Prog. Theor. Phys. Suppl. **89**, 1 (1986).

[18] K. Nagamine and M. Kamimura, Advanced in Nuclear Physics, **24**, 151 (1998).

[19] M. Kamimura, Prog. Theor. Phys. Suppl. **62**, 236 (1977).

[20] L.R. Suelzle *et al.*, Phys. Rev **162**, 992 (1967).

[21] B. Jenny *et al.*, Nucl. Phys. **A397**, 61 (1983).

[22] W. Gruebler *et al.*, Nucl. Phys. **A242**, 265 (1975).

[23] D.D. Clayton, *Principles of Stellaer Evolution and Nuclear Synthesis* (The University of Chicago Press, 1983).

[24] W. M. Yao *et al.* [Particle Data Group], J. Phys. G **33** (2006) 1.

[25] T. Asaka, K. Hamaguchi and K. Suzuki, Phys. Lett. B **490** (2000) 136 [arXiv:hep-ph/0005136].
M. Fujii, M. Ibe and T. Yanagida, Phys. Lett. B **579** (2004) 6 [arXiv:hep-ph/0310142].

[26] W. Buchmuller, K. Hamaguchi, M. Ibe and T. T. Yanagida, arXiv:hep-ph/0605164.

[27] W. Buchmuller, P. Di Bari and M. Plumacher, Annals Phys. **315** (2005) 305 [arXiv:hep-ph/0401240];
See, for a review, W. Buchmuller, R. D. Peccei and T. Yanagida, Ann. Rev. Nucl. Part. Sci. **55** (2005) 311 [arXiv:hep-ph/0502169].